Publications of the Astronomical Society of the Pacific
94:444–452, June 1982

# A CATALOG OF DIFFUSE NEBULAE AND EMISSION-LINE STARS IN NGC 6822

ROSEMARY M. KILLEN AND REGINALD J. DUFOUR*

Department of Space Physics and Astronomy, Rice University, P.O. Box 1892, Houston, Texas 77001

*Received 1981 July 11, revised 1982 February 8*

A catalog of 31 diffuse nebulae and 36 stellar emission-line objects in the Local Group irregular galaxy NGC 6822 is represented. Identifications of the objects were made from several wide-band and interference filter plates of NGC 6822 obtained with the CTIO 4-m telescope at the prime focus under conditions of excellent seeing. The numbers and sizes of the diffuse nebulae in NGC 6822 are similar to those of the population of H II regions in the Small Magellanic Cloud. The 36 stellar emission-line objects found in NGC 6822 appear to be emission-line stars, small H II spheres, and planetary nebulae.

*Key words:* diffuse nebulae—emission-line objects—galaxies—Local Group

## I. Introduction

During the early phases of a spectrophotometric study of emission-line nebulae and stars in the Local Group irregular galaxy NGC 6822 (Dufour and Talent 1980; Talent 1981; Dufour, Kirsch, and Talent 1982) it became desirable to obtain deep plates of the galaxy in H$\alpha$ and possibly other emission lines in order to identify objects in the galaxy suitable for further study. Several deep plates were taken for this purpose with the 4-m telescope at Cerro Tololo in 1976. This paper presents the results of the analysis of these plates in the form of a catalog of objects in NGC 6822 which are believed to be H II regions, planetary nebulae, emission-line stars, and, at least one case, supernova remnants.

The first identification of H II regions in NGC 6822 was made by Hubble (1925), who identified five objects. Subsequently, Hodge (1969, 1977) identified 16 nebulae. Sedwick and Ford (1976) report the identification of 55 emission-line objects, but details of that study have not been published to date. In addition, Kinman, Green, and Mahaffey (1979) have published identifications and spectroscopy of three compact H II regions in NGC 6822 missed in Hodge's surveys. Some physical data on the brighter H II regions in NGC 6822 are also available. Boggess (1967) derived luminosities, electron densities, and masses for the four most prominent H II regions using H$\alpha$ isophotometry. The spectra and chemical composition of several nebulae have been studied by Peimbert and Spinrad (1970), Smith (1975), Lequeux et al. (1979); Kinman, Green, and Mahaffey (1979); Pagel, Edmunds, and Smith (1980), Talent (1981), and by Dufour, Kirsch, and Talent (1982). Moreover, Dufour and Talent (1980) have analyzed the spectrum of a planetary nebula in NGC 6822 during the early phase of this study.

This catalog gives identifications, positions, and other data on 67 emission-line objects in NGC 6822—31 resolvable (diameters > 2 arc sec) diffuse nebulae (H II regions or supernova remnants) and 36 stellar objects (e.g., emission-line stars, planetary nebulae, or compact H II regions with diameters ⩽ 2 arc sec).

## II. Observations and Techniques

Several plates of NGC 6822 were obtained by one of us (R.J.D.) in June 1976, using the CTIO 4-m telescope at prime focus. Three additional 4-m plates were subsequently made available to us by S. van den Bergh of the Dominion Astrophysical Observatory. This plate material is listed in Table I. All of the plates were taken under conditions of excellent to good seeing (< 1–2 arc sec) and have photometric spot calibrations.

Plates 2016 and 2131 were taken through a five-inch square λ6560 interference filter of 120 Å FWHM. They were used to identify objects emitting H$\alpha$ and [N II] λλ6548, 6583. Plate 2118, taken through a similar interference filter centered at λ5000 (70 Å FWHM), was used to identify objects with strong [O III] λ5007 emission. Plate 2143, a baked IIIa-J plate taken through a GG495 filter with an effective bandpass of λλ5050–5500, was used as a "continuum" plate to compare the brightness of stellar objects against their brightness on the H$\alpha$ and [O III] plates. Plate 2009 (103a-D + GG495) was also useful as a continuum plate.

Diffuse or resolved nebulae were identified using high-contrast prints of the plates. All objects classified as "diffuse" had image diameters greater than 2 arc seconds and were clearly distinguishable from nonsaturated stellar images. The area studied was a 26 arc-minute diameter field centered on the galaxy. While most of the diffuse nebulae were readily apparent on the prints of both of the H$\alpha$ plates and on the [O III] plate, several of the fainter nebulae were visible only on the H$\alpha$ plates. This is partly due to the fact that the H$\alpha$ plates go deeper than the [O III] plate and partly because some of the faint nebulae are of rather low excitation. In order for a

*Visiting Astronomer, Cerro Tololo Inter-American Observatory, supported by the National Science Foundation under contract AST 74-04128.

TABLE I

PHOTOGRAPHIC PLATE MATERIAL
(All taken with CTIO 4 m f/2.7 Prime Focus)

| Plate # | Emulsion | Filter | Exposure (min.) | Seeing $\pi$ | Observer | Date | Comments |
|---|---|---|---|---|---|---|---|
| 2008 | 103a-O | GG385 | 7 | 1.5 | SvdB | 27/4/76 | Used for astrometry |
| 2009 | 103a-D | GG495 | 15 | 1.5 | SvdB | 27/4/76 | Backup "continuum" plate |
| 2016 | 098-04 | $\lambda$6560/120 | 75 | 1 | SvdB | 28/4/76 | Backup H$\alpha$ plate |
| 2117 | IIIa-J | GG385 | 45 | <1 | RJD | 21/6/76 | Used in checking "stellar" objects |
| 2118 | IIIa-J | $\lambda$5000/70 | 75 | 1-2 | RJD | 21/6/76 | [O III] plate |
| 2131 | 127-02 | $\lambda$6560/120 | 150 | 1.5 | RJD | 22/6/76 | Primary H$\alpha$ plate |
| 2143 | IIIa-J | GG495 | 20 | 1 | RJD | 23/6/76 | Primary "Continuum" plate |

nebula to be included in the list it had to be evident on at least both H$\alpha$ plates.

Stellar emission-line objects with both [O III] and H$\alpha$ emission were identified by comparing the brightness of stars on the [O III] and H$\alpha$ plates against the continuum plates (initially plates 2143 and 2117). The identification of stellar emission-line objects of lower excitation (showing only H$\alpha$ emission) was more problematical. Lack of a good red continuum plate caused some difficulties in discerning very red stars from weak H$\alpha$ objects. In our preliminary search we identified over a hundred possible H$\alpha$ objects. Using the $V$ (103a-D + GG495) plate (2009) taken by van den Bergh as a continuum comparison plate and setting the requirement that an H$\alpha$ object must be significantly brighter on the H$\alpha$ plates than on the $V$ plate, we selected those objects in the catalog. This procedure may have resulted in omission of some of the weaker H$\alpha$ objects, such as red supergiant stars.

In searching for stellar emission-line objects we used color-coded photographs of the galaxy made from the registered images of three positive transparencies: one of the H$\alpha$ plates (2131, coded red), the [O III] plate (2118, coded blue), and a continuum plate (2143, coded green). This procedure is analogous to that used by Dufour and Goodding (1975) to construct color photographs of galaxies from $B$, $V$, and $R$ plates. The color levels were adjusted so that continuum objects (normal stars) appeared white, strong H$\alpha$ objects appeared red, and strong [O III] objects appeared blue or magenta, depending on the relative strengths of [O III] and H$\alpha$. The resulting color photographs were not only useful for identifying the emission-line objects, but also for estimating the excitation ([O III]/ H$\alpha$ ratio) level for both the stellar objects and the diffuse nebulae.

It is important to mention that while our procedures seem to work well in identifying "stellar" emission-line objects that do not have saturated images on the plates, they generally fail for stellar objects with saturated images (roughly brighter than $B = 18$). Our original catalog did not contain three bright (by our standards) compact H II regions in NGC 6822 discovered by Kinman, Green, and Mahaffey (1979), which all have saturated, essentially stellar, images on our plates. (We thank the referee of an earlier draft of this paper for noting this fact.) While two of these objects ($\beta$ and $\gamma$ in their paper) were marked as possible stellar emission-line objects in our preliminary searches, they were subsequently discarded from our list because their saturated images on the H$\alpha$, [O III], and continuum plates prevented definitive identification as emission-line sources. For completeness, we have included them in our list, with the note that other similarly "bright" stellar emission-line objects in NGC 6822 may have escaped our search.

The positions and brightnesses of the objects in the catalog were measured on plate 2008 using an Optronics International Specscan S-3000 microdensitometer. Stellar objects were centered in a 50-$\mu$m (0.93 arc sec) circular aperture and the position, in microns, and density were measured. For diffuse objects the positions of their apparent centers or that of the apparent exciting star near the centers were measured. The microdensitometer has a positional accuracy of $\pm$ 1 $\mu$m. Repeated measurements of the positions of the same stellar objects over three separate periods indicated a repeatability of better than $\pm$ 10 $\mu$m in most cases. The repeatability of the density reading was $\pm$ 0.02 $D$ in most cases.

## III. The Catalog

Tables II and III list, respectively, the 31 diffuse nebulae and the 36 stellar emission-line objects identified in

TABLE II
DIFFUSE NEBULAE

| ID | α(1950) | δ(1950) | Size (arc sec) | S(Hα) | Excitation | Hodge (1977) |
|---|---|---|---|---|---|---|
| D1 | $19^h41^m42^s.0$ | -14°29'17" | 59x40 | 120 | VH-L | 2 |
| D2 | 19 41 42.4 | -14 51 58 | 43x26 | 65 | L | 3 |
| D3 | 19 41 42.6 | -14 51 28 | 50x34 | 20 | H | 1 |
| D4 | 19 41 44.4 | -14 49 38 | 56x53 | 75 | M-L | 4 |
| D5 | 19 41 44.4 | -14 49 48 | 3x3 | 50 | M | |
| D6 | 19 41 45.2 | -14 49 47 | 5x4 | 75 | H | |
| D7 | 19 41 48.2 | -14 58 25 | 53x34 | 65 | VH | 5 |
| D8 | 19 41 48.8 | -14 59 07 | 16x12 | 20 | H | |
| D9 | 19 41 58.6 | -14 51 11 | 13x13 | 30 | M | |
| D10 | 19 41 58.7 | -14 51 35 | 16x12 | 70 | H-M | 6 |
| D11 | 19 41 58.7 | -14 53 32 | 23x17 | 25 | L | 7 |
| D12 | 19 41 59.5 | -14 50 37 | 28x12 | 30 | M | |
| D13 | 19 42 00.3 | -15 00 15 | 5x4 | 220 | M | |
| D14 | 19 42 01.0 | -15 00 06 | 5x3 | 40 | L | |
| D15 | 19 42 01.1 | -15 00 13 | 3x2 | 60 | L | |
| D16 | 19 42 01.5 | -15 00 06 | 6x3 | 170 | L | 8 |
| D17 | 19 42 01.7 | -15 00 04 | 6x5 | 550 | M | 8 |
| D18 | 19 42 02.7 | -14 59 15 | 6x6 | 190 | H | 10 |
| D19 | 19 42 03.2 | -14 50 28 | 40x30 | 1600 | H-M | 9 |
| D20 | 19 42 03.4 | -14 55 53 | 15x11 | 20 | M | |
| D21 | 19 42 04.2 | -14 50 22 | 18x15 | 35 | M-L | |
| D22 | 19 42 06.4 | -14 57 48 | 9x7 | 35 | L | |
| D23 | 19 42 07.2 | -14 55 45 | 7x7 | 70 | L | 12 |
| D24 | 19 42 08.0 | -14 54 41 | 28x12 | 25 | L | |
| D25 | 19 42 12.7 | -14 54 10 | 40x33 | 20 | M | |
| D26 | 19 42 15.6 | -14 50 31 | 59x53 | 520 | H-L | 14 |
| D27 | 19 42 15.9 | -15 04 49 | 8x8 | 25 | L | |
| D28 | 19 42 16.5 | -15 04 29 | 35x27 | 20 | L | |
| D29 | 19 42 18.2 | -14 55 52 | 13x11 | 25 | M | |
| D30 | 19 42 21.1 | -14 56 06 | 45x34 | 25 | M | 15 |
| D31 | 19 42 26.2 | -14 52 48 | 26x22 | 30 | H | 16 |

this survey. Identifications of the diffuse nebulae are presented in Figure 1, which is a high-contrast print of plate 2131 (150-minute exposure Hα plate). The identifications of the stellar emission-line objects are presented in Figures 2a and 2b, which show, respectively, the northern and southern halves of NGC 6822 from medium contrast prints of plate 2117 (45-minute exposure IIIa-J + GG385 plate).

In Table II we list for each nebula the 1950.0 coordinates of their centers obtained from the measured $X,Y$ positions. These positions were transformed to right ascension and declination using a linear least-squares fit of the positions and coordinates of five SAO stars. The $X,Y$ positions of these and of the catalog objects were adjusted for the geometric field distortion of the CTIO 4-m prime-focus UBK-7 corrector using correction formulae of Chiu (1976) developed for the KPNO UBK-7 corrector. The absolute rms errors of the transformed coordinates are estimated to be $\pm$ $0^s.1$ in right ascension and $\pm$ $1''$ in declination. The angular sizes in arc seconds of the major and minor axes of the nebula are also listed. These are believed to be accurate within a few seconds of arc for the brighter nebulae, but reflect much personal discretion in determination of the boundary of the faint or complex nebulae. Table II also gives a relative intensity scale of the Hα surface brightness of the brightest region of each nebula. The density was measured through a 0.93 arc second circular aperture on plate 2131 and transformed to relative intensity using the spot calibration exposed on the plate. A crude calibration of these intensities has been extrapolated from spectrophotometry of several of the nebulae by Talent (1981). Assuming that the [N II] lines have negligible intensities relative to Hα, we find that:

$$F(\mathrm{H}\alpha) = 2.3S(\mathrm{H}\alpha) \times 10^{-17}\ \mathrm{ergs\ s^{-1}\ arc\ sec^{-2}\ cm^{-2}} \quad .$$

An estimate of the excitation level obtained from the color hue of objects on the color composite photographs is also presented in the sixth column. The visual criteria for the codes are:

VH: very high: [O III] $\gg$ Hα (blue color)

H: high: [O III] $>$ Hα (magenta color)

TABLE III
STELLAR EMISSION-LINE OBJECTS

| ID | α(1950) | δ(1950) | B | Excitation | Type |
|---|---|---|---|---|---|
| S1 | $19^{h}41^{m}40^{s}.9$ | -14°48'56" | 18.6 | H | star |
| S2 | 19 41 41.2 | -14 55 41 | 17.9 | H | H II |
| S3 | 19 41 42.6 | -14 49 23 | 20.0 | H | star |
| S4 | 19 41 42.6 | -14 51 29 | 21.8 | M | star |
| S5 | 19 41 43.2 | -14 54 46 | 18.4 | H | H II |
| S6 | 19 41 45.2 | -14 49 43 | 20.8 | H | star |
| S7 | 19 41 45.4 | -14 48 05 | 20.5 | L | H II |
| S8 | 19 41 47.8 | -15 03 19 | 19.6 | L | star |
| S9 | 19 41 48.2 | -14 58 12 | 19.9 | VH | H II |
| S10 | 19 41 53.1 | -14 57 48 | 22.3 | H | PN? |
| S11 | 19 41 58.7 | -14 59 45 | 17.4 | H | H II |
| S12 | 19 41 59.5 | -14 50 37 | 21.0 | H | H II |
| S13 | 19 42 59.5 | -14 59 49 | 20.2 | L | H II |
| S14 | 19 41 59.9 | -14 53 47 | 22.8 | VH | PN? |
| S15 | 19 42 00.0 | -15 00 15 | 21.0 | L | H II |
| S16 | 19 42 00.1 | -14 55 22 | 22.8 | H | PN? |
| S17 | 19 42 01.0 | -15 00 09 | 22.0 | L | H II |
| S18 | 19 42 01.2 | -14 59 34 | 20.2 | H | star |
| S19 | 19 42 01.4 | -15 00 11 | 19.2 | H | star |
| S20 | 19 42 01.5 | -15 00 04 | 21.2 | L | H II |
| S21 | 19 42 01.6 | -14 50 21 | 19.6 | M | star |
| S22 | 19 42 03.7 | -14 50 32 | 20.0 | L | H II |
| S23 | 19 42 03.9 | -14 58 11 | 21.9 | H | PN? |
| S24 | 19 42 04.3 | -14 50 27 | 19.5 | M | star |
| S25 | 19 42 04.9 | -14 55 23 | 21.2 | L | star |
| S26 | 19 42 05.5 | -14 51 02 | 22.4 | M | PN? |
| S27 | 19 42 06.3 | -14 55 49 | 21.3 | H | star |
| S28 | 19 42 07.6 | -14 55 07 | 20.0 | H | star |
| S29 | 19 42 07.8 | -14 53 14 | 22.5 | L | H II (or PN) |
| S30 | 19 42 11.8 | -14 48 53 | 21.7 | VH | PN? |
| S31 | 19 42 14.8 | -14 50 40 | 19.8 | H | star |
| S32 | 19 42 15.4 | -15 04 48 | 19.3 | H | star |
| S33 | 19 42 17.6 | -14 54 46 | 22.5 | H | PN! |
| S34 | 19 42 20.8 | -14 55 57 | 20.6 | M | H II |
| S35 | 19 42 21.0 | -15 01 45 | 21.2 | L | H II |
| S36 | 19 42 27.6 | -14 52 44 | 20.1 | M | H II |

M: moderate: [O III] < Hα (orange color)

L: low: no [O III] detected (red color) .

From the data of Talent (1981) these roughly correspond to observed λ5007/Hα ratios of $\gtrsim$ 1.3 for VH, ~ 0.9–1.2 for H, ~ 0.4–0.8 for M, and $\lesssim$ 0.3 for L. Finally, in the seventh column of Table II, we present cross references to the designations of H II regions in NGC 6822 by Hodge (1977). Note that the numbering system in Hodge (1977) differs from that used in his earlier atlas (Hodge 1969), but the H II regions are the same.

Most of the diffuse nebulae in Table II are isolated objects excited by one or more prominent blue stars. Several appear in associations of early-type stars cataloged by Hodge (1977). A few of the nebulae (e.g., D5, D6, and D21) are bright knots excited by a single star within a larger nebula. D5 and D6 are within the prominent ring nebula, D4, but the two have a considerably higher excitation than the D4 nebula as a whole. In such situations where there are bright resolved knots of nebulosity apparently produced by a particular star within a larger nebula complex (usually around an association of stars), we have chosen to give the knots separate designations. The diffuse nebulae show a great diversity of structure and excitation. Several, such as D2, D5, and the southern parts of D26 apparently are low-to-medium excitation ring-like ionization-front structures around prominent blue stars or associations. Other nebulae, such as D1 and D7, are of very high excitation and have a smooth appearance in [O III]. The bright knot in the northern part of D1 shows a remarkable gradient in excitation from high in the southern part near a bright blue star to low

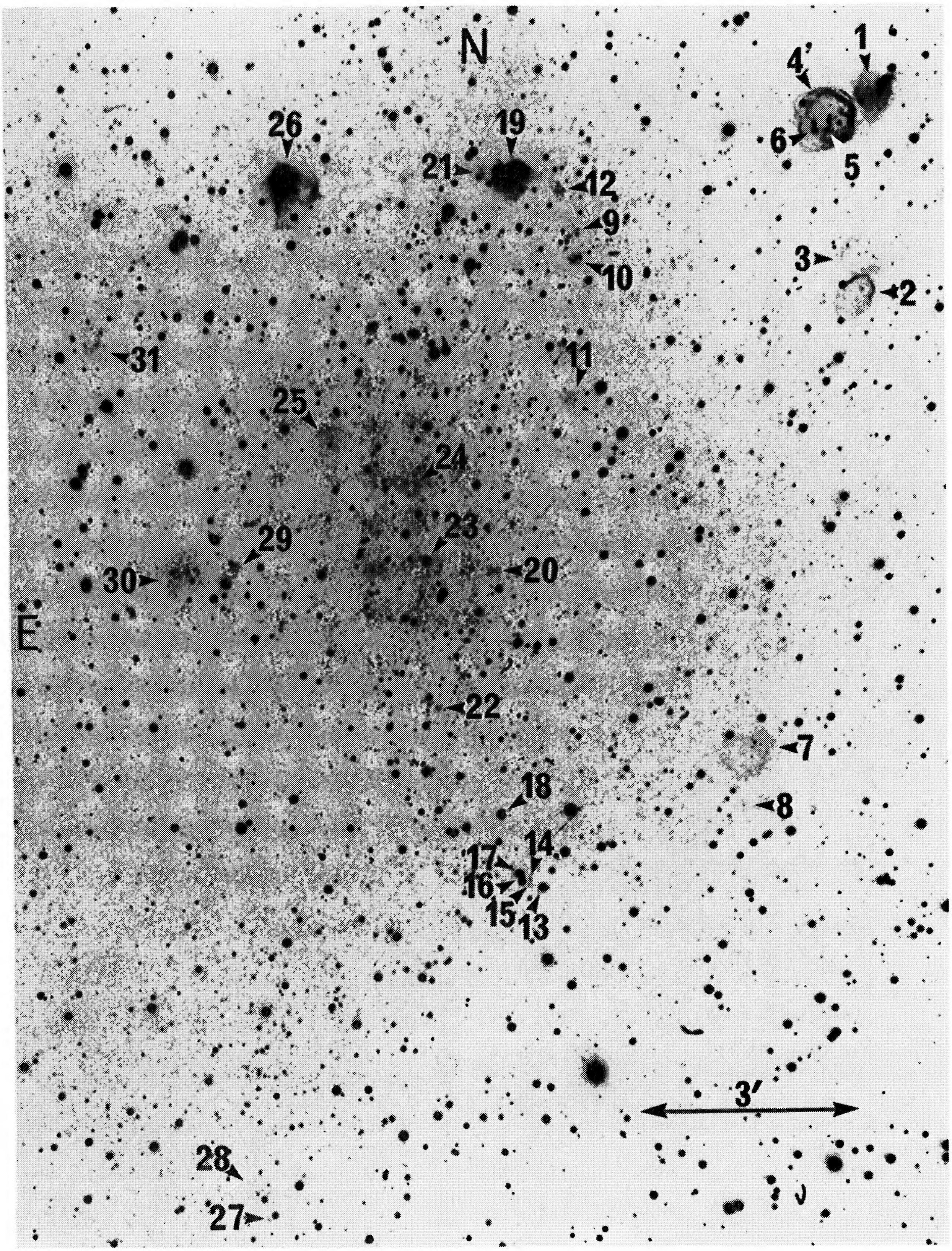


FIG. 1—Identifications of diffuse nebulae in NGC 6822 listed in Table II. Photograph is a high-contrast print from plate 2131 (150-minute exposure, 127-02 emulsion + λ6560/120 Å FWHM filter) taken with the CTIO 4-m telescope at prime focus.

along the northern boundary. The nebula, D23, located in the central part of the main body of NGC 6822, has a knotty ring-line structure of low excitation throughout without an apparent central ionizing source. This makes D23 a plausible candidate for a supernova remnant.

We confirm 14 of the 16 H II regions identified by Hodge (1969, 1977) using lower resolution 1.2-m Schmidt plates. Hodge nos. 11 and 13 in his 1977 numbering system are apparently not H II regions, but are two unresolved red stars on his plate and a plate flaw, respectively. In addition, we have identified 17 new H II regions in NGC 6822.

The objects listed in Table III are defined to be emission-line objects that appear to be essentially unresolved on all of our plates. Generally we designated an emission-line object as "stellar" if its circular image as a nonsaturated density profile with FWHM indistinguishable from unsaturated stars on the same plate (typically FWHM $< 2$ arc sec). If we assume a distance of 0.56 Mpc for NGC 6822 (de Vaucouleurs 1978), this corresponds to a spatial resolution of 5.4 pc in the galaxy. Planetary nebulae and small H II spheres would therefore not be resolved.

As for the diffuse nebulae, we give 1950.0 coordinates and the excitation level for the stellar emission-line objects in Table III. The coordinates are believed to be accurate to $\pm$ 2 arc seconds. Also given are approximate $B$ magnitudes of these objects and of nine stars in NGC 6822 which have *UBV* photometry published by Hodge (1977). Magnitudes were obtained by measuring the central image densities on plate 2008 using a 0.37 arc second circular aperture on the Specscan microdensitometer. The densities were converted to relative intensities using the calibration spots on the plate and then were transformed to $B$ magnitudes by interpolation of a least-squares fit between the logarithm of the relative intensities and the $B$ magnitudes of the nine Hodge stars. This procedure, although crude, gave a surprisingly good fit to the nine standard stars. The suggested rms errors in $B$ over the range $18 \lesssim B \lesssim 21$ is less than 0.1 magnitude. The errors for fainter objects ($B > 22$) may be significantly larger, possibly as much as $\pm$ 0.2 magnitude.

For consistency we include data on the three compact H II regions of Kinman, Green, and Mahaffey (1979) in Table III, although the (saturated) images are unresolved on our plates. Their objects $\alpha$, $\beta$, and $\gamma$ are, respectively, designated as S2, S5, and S11 in the table. We also give magnitudes and positions of the three objects using data from their paper in the table, since the brightnesses of the saturated images are difficult to measure reliably on our plates. A quick check of the positions agree with their results to within $\pm$ 3 arc seconds in all cases.

Our detection limit for stellar emission-line objects seems to be near $B \sim 22.8$, but this depends on the H$\alpha$ and [O III] flux more than on the $B$ magnitude. The planetary nebula observed by Dufour and Talent (1980) (object S33 in Table III) has $B = 22.5$, but is prominent on both of the H$\alpha$ and [O III] plates. According to their study, this object has $F$ (H$\alpha$ + [N II]) $= 1.8 \times 10^{-14}$ ergs cm$^{-2}$ s$^{-1}$ and $F$ ($\lambda$5007) $= 1.8 \times 10^{-14}$ ergs cm$^{-2}$ s$^{-1}$ for observed fluxes above the atmosphere. Comparison of its image intensity on the [O III] and H$\alpha$ plates with several of the faintest stellar objects in the catalog suggests that our detection limit for stellar emission-line objects with weak continuum is about $3 \times 10^{-15}$ ergs cm$^{-2}$ s$^{-1}$ for both [O III] $\lambda$5007 and H$\alpha$ (+[N II]).

In the sixth column of Table III we have classified the stellar emission-line objects into three categories: "star" for an emission-line star, "H II" for a small H II sphere, and "PN?" for a planetary nebula candidate. These classifications are our best guesses based on their $B$ magnitude, excitation level, and the relative prominence of the continuum to the line emission, Objects classified as stars have a prominent continuum in addition to the line emission and are brighter than $B = 22$. Objects classified as planetary nebula candidates have high excitation (i.e., show both H$\alpha$ and [O III] in substantial strength above the continuum) and have $B \gtrsim 22$; which implies that their absolute blue magnitudes are fainter than $M_B \approx -2.5$ given a distance modulus of NGC 6822 of $\langle \mu_B \rangle = 24.5$ (de Vaucouleurs 1978). This limit is comparable to the absolute blue magnitudes of the brightest planetary nebulae in the Magellanic Clouds. Objects classified as H II spheres have H$\alpha$ emission substantially greater than that of the continuum or marginal resolution on some plates. Generally they have $B < 22$. One object, S29, may be either an H II sphere or a low-excitation planetary nebula. Most of the objects classified as H II spheres appear in or near diffuse nebulae.

## IV. Discussion

The distribution of diffuse nebulae in NGC 6822 consists of three general aggregations. By far the most prominent is in an "arm" along the northern perimeter of the galaxy, with D1 at the west end and D31 at the east end. This group follows a rough east-west line and includes the two most prominent H II regions in NGC 6822, D19, and D25, as well as several of the most prominent OB associations found by Hodge (1977). A second group, containing several large nebulae of generally low surface brightness, lies in the central region of the galaxy with D11 on the west end and D30 on the east end. Only D30 is obviously associated with a prominent OB association. Most of these nebulae are apparently excited by a single blue star. The third group of nebulae lies in the southern "arm" of the galaxy, beginning with D7 and D8 on the west end, trailing southeast through the D13–D18 complex of small H II regions of high surface brightness, and terminating at D27 and D28 in the east. While this arm

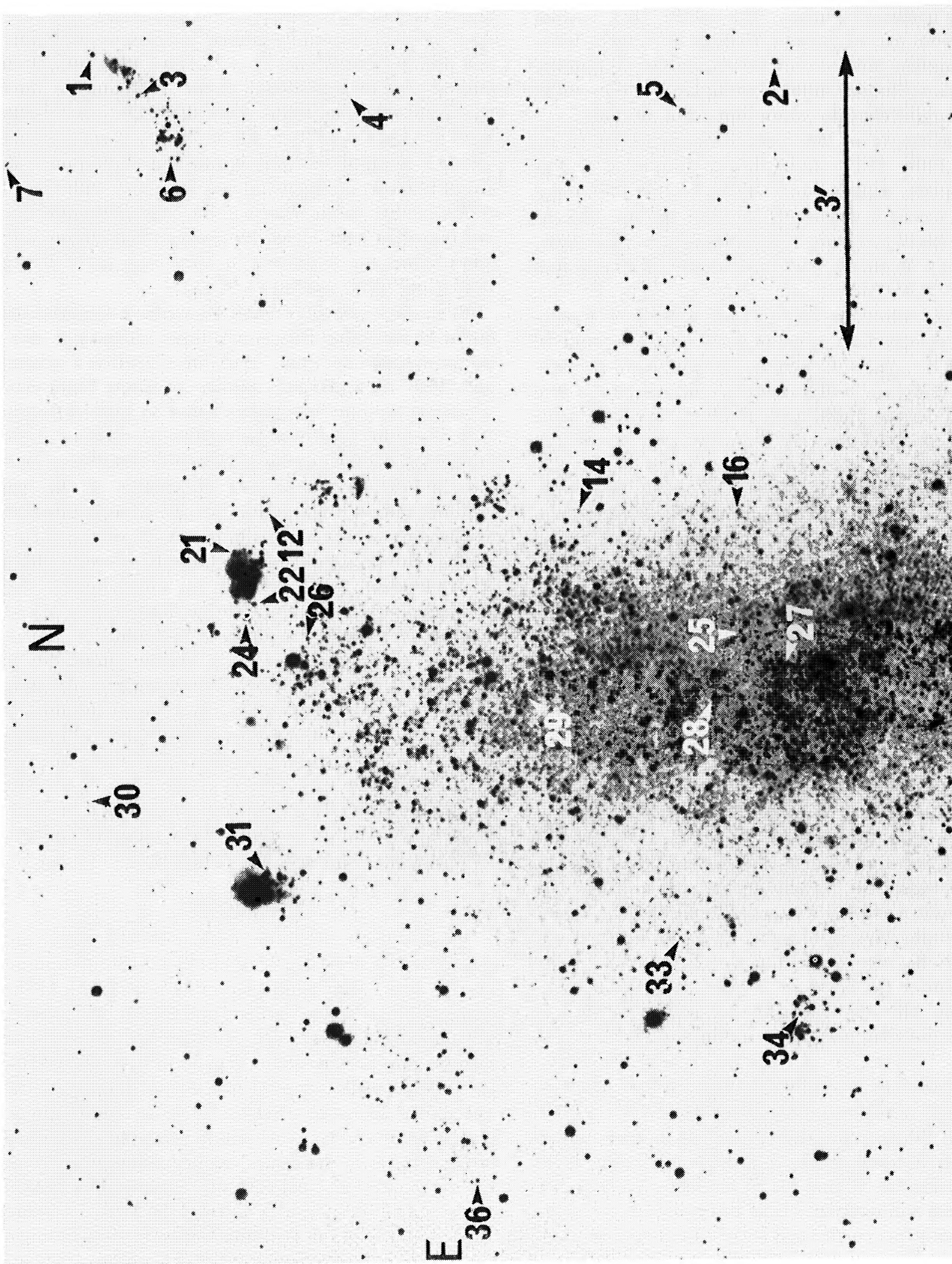


FIG. 2a—Identifications of stellar emission-line objects in the northern half of NGC 6822. Photograph is a print from plate 2143 (45-minute exposure, baked IIIa-J emulsion + GG385 filter) processed to show only stars brighter than $B \sim 23$.

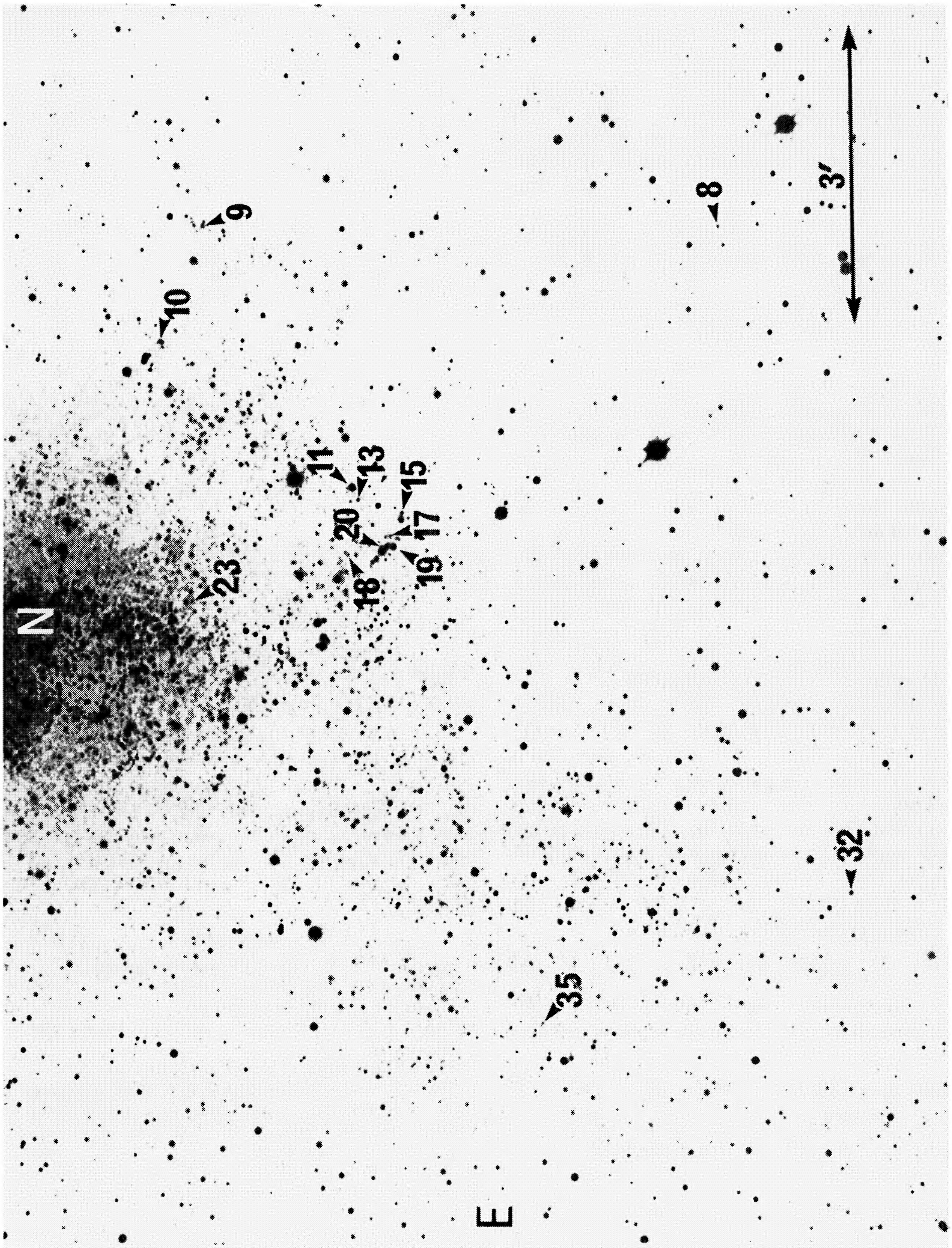


FIG. 2b—Identifications of stellar emission-line objects in the southern half of NGC 6822 from plate 2143.

is characterized by numerous blue stars (compare Figs. 1 and 2), it does not have the large "hot beds" of star formation and H II regions like the northern arm.

The distribution of stellar emission-line objects is similar to that of the diffuse nebulae. This is to be expected if most are H II spheres or young hot shell stars. Most of the planetary nebulae candidates are located in or near the central main body of the galaxy, suggesting that NGC 6822 does not have an extended population of intermediate-age stars significantly set apart from the main body of the galaxy (which is roughly north to south between the two "arms").

Figure 3 shows the distribution of the mean diameters of the diffuse nebulae in NGC 6822. These were computed from the average apparent angular size of the major and minor axes of each nebula and then converted to mean diameters in parsecs using a distance of 0.56 Mpc for NGC 6822 (de Vaucouleurs 1978). The nebulae were binned into 25-pc intervals for this purpose. We also give the distributions of the mean diameters of H II regions in the Large and Small Magellanic Clouds using the tabulated data on their sizes from Henize (1956) and distances of 0.046 Mpc and 0.053 Mpc for the LMC and SMC, respectfully (de Vaucouleurs). For comparative equality with our data, all H II regions in the Clouds with a mean diameter less than 5 pc were excluded from the counts and the large complexes in the LMC were grouped together and counted as one nebula.

From the figure it is apparent that the total number of H II regions in NGC 6822 is more like the SMC then the LMC. However, the slope of the size distribution of H II regions in NGC 6822 is less steep than for the SMC and more similar to that of the LMC. Also, the largest H II regions in NGC 6822 are larger than the largest in the SMC, but significantly smaller than the huge complexes found in the LMC. The distribution of sizes of H II regions in all three galaxies over the 5–200 parsec range can be described rather well by the expression:

$$\log N = A + BD \quad , \qquad (1)$$

where $N$ is the number in each 25-pc bin and $D$ is the mean diameter in parsecs. For the three galaxies we obtain:

NGC 6822: $A = 1.07, B = -\ 6.0 \times 10^{-3}$, $r = 0.94$ ;

SMC: $A = 1.46, B = -\ 10.3 \times 10^{-3}$, $r = 0.92$ ;

LMC: $A = 1.64, B = -\ 7.4 \times 10^{-3}$, $r = 0.91$ ;

where $r$ is the statistical linear correlation coefficient.

These data show that the population of H II regions in NGC 6822 has numbers and sizes rather more similar to the SMC than the LMC. This is not surprising since many of the integrated properties of the SMC and

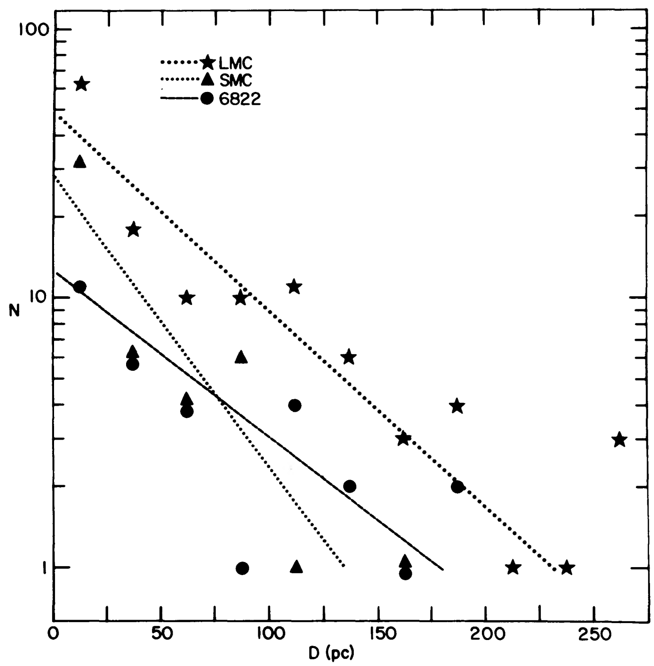


FIG. 3—Distribution of mean diameters of H II regions in NGC 6822, SMC, and LMC. Lines show least-squares linear regressions to the distributions as discussed in the text.

NGC 6822 are similar (see, for example, the tabulation in Talent (1981)). The similarity of H II region populations suggest that the current star-formation activity in the two galaxies may be similar.

We should like to express our gratitude to the staff of CTIO for their help with the observations and to Dr. S. van den Bergh for loaning us his excellent plates. Mr. R. A. Goodding of Technicolor Graphics, Inc., at the NASA L. B. Johnson Space Center made the color composites which aided us much in this study. This research was supported in part by NSF grants AST 77-27214 and AST 80-07450 to Rice University.

## REFERENCES

Boggess, N. 1967, Ph.D. Thesis, University of Michigan.
Chiu, Liang-Tai G. 1976, *Pub. A.S.P.* 88, 803.
de Vaucouleurs, G. 1978, *Ap. J.* 223, 730.
Dufour, R. J., and Goodding, R. A. 1975, *Proc. SW Regional Conf. Astr. Ap.* 1, 71.
Dufour, R. J., and Talent, D. L. 1980, *Ap. J.* 235, 22.
Dufour, R. J., Kirsch, R. M., and Talent, D. L. 1982 (in preparation).
Henize, K. G. 1956, *Ap. J. Suppl.* 2, 315.
Hodge, P. 1969, *Ap. J. Suppl.* 18, 73.
——— 1977, *Ap. J. Suppl.* 33, 69.
Hubble, E. P. 1925, *Ap. J.* 62, 409.
Kinman, T. D., Green, J. R., and Mahaffey, C. T. 1979, *Pub. A.S.P.* 91, 749.
Lequeux, J., Peimbert, M., Rayo, J. F., Serrano, A., and Torres-Peimbert, S. 1979, *Astr. and Ap.* 80, 155.
Pagel, B. E. J., Edmunds, M. G., and Smith, G. 1980, *M.N.R.A.S.* 193, 219.
Peimbert, M., and Spinrad, H. 1970, *Astr. and Ap.* 7, 311.
Sedwick, K. E., and Ford, H. C. 1976, *Bull. A.A.S.* 8, 568.
Smith, H. E. 1975, *Ap. J.* 199, 591.
Talent, D. L. 1981, Ph.D. Thesis, Rice University.